journal

J. Am. Ceram. Soc., 76 [10] 2555–60 (1993)

Atomic Force Microscopy and X-ray Photoelectron Spectroscopy Investigation of the Onset of Reactions on Alkali Silicate Glass Surfaces

Gregory I. Rudd,* Stephen H. Garofalini,* and David A. Hensley
Department of Ceramics, and Center for Ceramics Research and Interfacial Molecular Science Laboratory,
Rutgers University, Piscataway, New Jersey 08855

C. Mathew Mate
IBM Almaden Research Center, San Jose, California 95120

Atomic force microscopy was used to measure forces acting on a sharp tungsten tip as it was brought into contact with silica and 30 mol% binary alkali silicate glasses. Experiments were performed in controlled atmospheres and under vacuum. Attractive forces and liquid-layer thicknesses were found to vary markedly between the glasses, and heterogeneity was observed on the binary alkali silicates analyzed *in vacuo*. Air or wet carbon dioxide exposure resulted in the penetration of the tip into a soft surface layer on the alkali silicates. In addition, liquid layer formation on the alkali silicates was found to be promoted by exposure to water vapor in the order lithium < sodium < potassium. X-ray photoelectron spectroscopy indicated that reaction between the potassium silicate surface and water vapor occurred on exposure to only 10^{-4} torr (1 torr = 1.33×10^2 Pa) water. Surface segregation and leaching of potassium occurred under the same conditions.

I. Introduction

ALKALI modifiers are used in the vast majority of commercially important silicate glass formulations to lower the working temperature of the glass. It has long been known, however, that increasing alkali content lowers the resistance to corrosion by aqueous solutions. Corrosion by aqueous solutions has motivated many studies of the surface properties of silicate glasses.[1] Glassmaking practice has found a balance between workability and durability with formulations of soda–lime–silica and potash–lime–silica glasses, often including small quantities of other network-forming cations, such as aluminum, to enhance a given property.[2] Although many compositions have been developed empirically, little is known about the detailed structure and chemistry of even simple glass surfaces on an atomic scale. Applications of various surface spectroscopies and computer simulations, however, have provided insight into the surface chemistry and structure of alkali silicate glasses.[3–6] Such insight is important for the study of glass chemical reactions, mechanical properties, and ionic conductivity.

Alkali silicate glasses containing greater than 16 mol% fraction of alkali oxide are especially susceptible to corrosion.[7] The solubility of silica increases rapidly at pH >9,[8] and, in some cases, it has been shown that the exposure of an alkali silicate glass to water results in a hydration layer with a pH high enough to cause dissolution of the network. Sodium and potassium silicate glasses undergo leaching and changes in surface structure, and reaction with wet carbon dioxide has been observed and quantified for some lithium-containing glasses.[9–10]

To provide a more detailed understanding of glass surfaces, we have investigated the surface properties of 30 mol% lithium, sodium, and potassium silicate glasses in ambient and controlled atmosphere and under vacuum by atomic force microscopy (AFM) using the "force–distance" (*F–D*) curve technique and by X-ray photoelectron spectroscopy (XPS). We have chosen these glasses because there has been a large number of experimental and computational studies of simple alkali silicate glasses to which we can refer.[11] These glasses are also of interest for AFM analysis because of possible nanoscale heterogeneity[12–16] which may exist at the surface and because of the different reactivities of the glasses with water. For comparison, we also have studied a pure silica glass.

For the *F–D* curve experiments, the forces between an AFM tip and a sample are measured as they are brought into contact and withdrawn. These experiments allow a measurement of forces due to van der Waals and repulsive interactions and the thickness of extremely thin liquid films.[17,18] By moving the sample between measurements, *F–D* curves can be obtained for various points on the surface. A representative *F–D* curve from pure silica is shown in Fig. 1. From such curves we can obtain the *onset distance* and the *attractive force* as the tip and sample approach, the *adhesive force* and the *break-free length* on withdrawal. These terms are defined in Fig. 1 and are expected to vary as the surface composition and contamination film on the surface varies.

II. Experimental Procedure

(1) Preparation of Glasses

Alkali silicate glasses were prepared from reagent-grade alkali carbonates and silica (Cab-o-Sil, Cabot Corp., Waltham, MA). The powders were ball-milled dry overnight, melted in silica crucibles at 1350°C, and poured into a steel mold. Cooling occurred at about 50°C/s. The sodium and potassium silicates were annealed at 600°C for 1 h; the lithium silicate proved necessary to be annealed at 450°C to avoid crystallization of lithium disilicate. The pure silica glass was commercially obtained (Amersil TO-8, Heraeus-Amersil, Duluth, GA).

(2) *F–D* Microscopy in Air and Controlled Atmosphere

In-air AFM was used as has been described previously.[19] Each tip and cantilever was fabricated from tungsten wire, 50 μm in diameter, in which one end was bent at right angle and

---

C. G. Pantano—contributing editor

Manuscript No. 194939. Received January 18, 1993; approved May 28, 1993.
Supported by a U.S. Department of Energy URIP Grant (No. DE-FG05-8975521) for the purchase of materials for the construction of a UHV-AFM; the work of SHG and DAH was supported in part by U.S. Department of Energy Grant No. DE-FG05-88ER-45368; and the travel of GIR was supported by IBM.

*Member, American Ceramic Society.

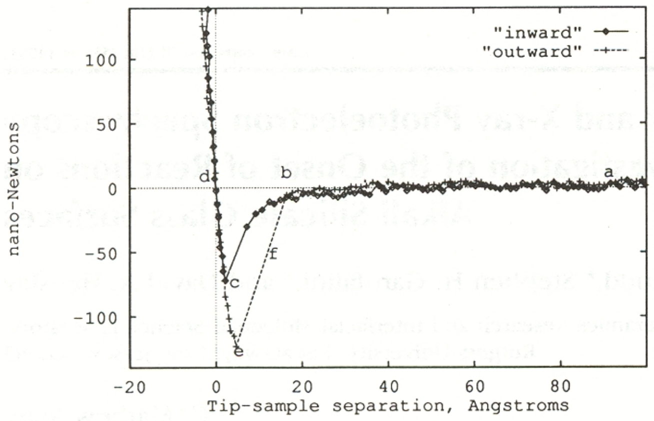

Fig. 1. Example of a *F–D* curve obtained on pure silica under vacuum. Repulsive forces are positive, attractive negative. "Inward" line traces the approach, "outward" withdrawal. At **a**, tip and sample are far apart and no force is measured. Around **b** onset of attraction begins, which is determined from the point where the slope of the attractive force crosses a threshold (about 1 nN/Å). At **c** attractive force reaches a maximum and repulsive forces initiate. At point **d** net force is again zero, and we define this as zero tip–sample separation. On withdrawal, the attractive force goes through a maximum at **e** and is called the "adhesive force." Break-free occurs along **f** and, for discussions in this paper, is the point where the force returns to zero.

electrochemically etched in potassium hydroxide solution to form a sharp tip, typically 100 to 500 Å (1 Å = 0.1 nm) in radius. The cantilever spring constants were determined from the measured vibration resonance frequency and ranged from 40 to 90 N/m. The force resolution of our apparatus in these experiments was better than 5 nN.

The AFM was enclosed in a box capable of being purged to produce a controlled atmosphere. The sample surfaces were prepared by fracturing the silicate glasses and were analyzed immediately after fracture. Samples analyzed under nitrogen and carbon dioxide atmospheres were fractured in a glove box under dry nitrogen and immediately transferred to the purged microscope box. Brief exposure (<1 min) to ambient atmosphere was unavoidable. Analysis was started within 10 min of transfer. We found the measurements made on freshly fractured, pure vitreous silica to be consistent under a given set of conditions and, therefore, used this to verify the quality of a tip.

(3) F–D Microscopy and XPS under Vacuum

We built two ultra-high-vacuum (UHV) AFM, *F–D* microscopes, one at Rutgers University and the other at IBM Almaden.[20] The AFM work presented here was performed on the latter instrument in a UHV chamber which was maintained at 2×10^{-7} torr (1 torr = 1.33×10^2 Pa) for these experiments. The experimental protocol was similar to that described above, with the exception that, for *in-vacuo* measurements, tips were cleaned by heating to >1000°C by electron bombardment. Samples analyzed *in vacuo* were fractured at 1×10^{-6} torr and transferred into the analysis chamber under vacuum in less than 1 min. Analysis was started within 20 min of transfer.

Surface spectroscopy was performed (Model XSAM 800, Kratos Analytical, Ramsey, NJ) using a sample exposure and preparation chamber with a fracture stage and XPS capability. The base pressure of the spectrometer chamber was 2×10^{-9} torr.

III. Results and Discussion

(1) AFM Results in Ambient, and Wet and Dry Nitrogen and Carbon Dioxide Atmospheres

Figure 2 shows typical *F–D* curves obtained after 1-h exposure to ambient atmosphere for pure silica (Fig. 2(A)) and for the sodium silicate glass (Fig. 2(B)). The two curves in Fig. 2 are dramatically different. For pure silica, the repulsive force increases quickly after the tip comes into contact with the sample and decreases reversibly when the sample is withdrawn, indicating a very stiff, elastic contact between the tip and the sample. For the sodium silicate glass, the attractive well is so small that it cannot be observed on the scale of the illustration. In addition, the repulsive force increases much less quickly on the sodium silicate glass after making contact, indicating a much less stiff surface. When the sodium silicate sample is withdrawn, the *F–D* curve is not reversible, indicating that some plastic deformation of the substrate has occurred. The distance that the curve has moved into the sample is the penetration depth of the tip into the sample and measures the degree of plasticity of the material at the glass surface. The separation distance at which the force crosses the zero axis upon withdrawal (~100 Å) is much different from the original zero location on approach. This indicates that the tip has plastically deformed the sodium silicate substrate surface and is now withdrawing from a surface which is ~100 Å below the original undeformed surface. Although we can argue that the tip is being deformed rather than the substrate, the same tip was used on pure silica without evidence of plasticity; also, continued use of the tip at different locations on the same substrate gives similar *F–D* curves, indicating that the tip had not been altered. Substantial penetration is also observed in the *F–D* curves for lithium and potassium silicate glasses in ambient atmosphere, increasing in the order lithium < sodium < potassium.

To explain the soft surfaces observed for the alkali silicate glasses in air, we hypothesize that the alkali ions in the silicate are reacting with the water vapor and carbon dioxide in the ambient atmosphere to form a liquid film and a soft hydrated

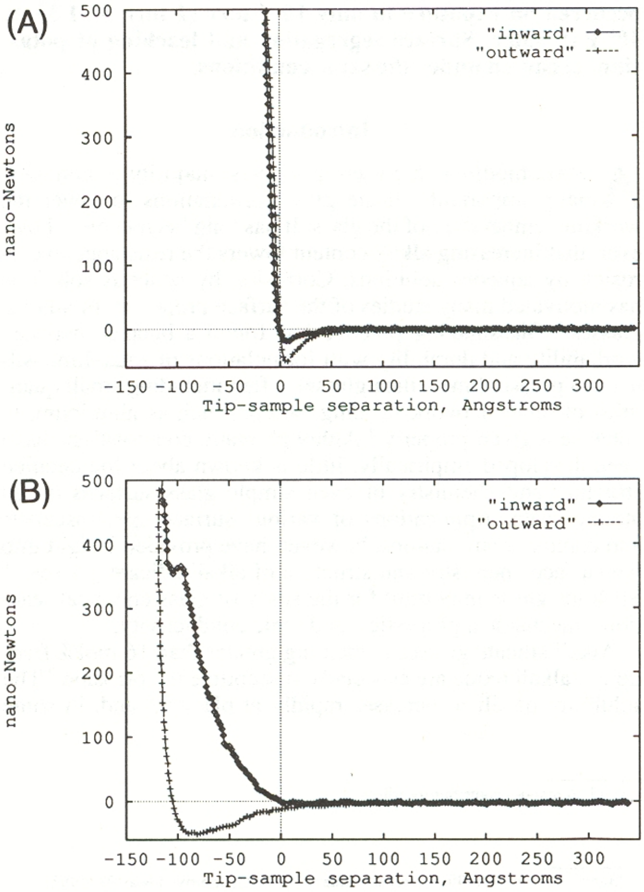

Fig. 2. (A) Example of a *F–D* curve obtained on pure silica in air. (B) Example of "mucky" *F–D* curve obtained on sodium silicate glass exposed to air 1 h. Penetration of the tip into the sample ("plasticity") and a long pull off are characteristic of a soft surface with an adsorbed liquid layer.

surface layer containing hydrates or carbonates on the glass surfaces. To test this hypothesis, we have measured the *F–D* curves for the alkali silicate glasses exposed to a variety of controlled atmospheres. Figure 3 shows typical *F–D* curves for lithium silicate glass. For lithium silicate in dry nitrogen (Fig. 3(A)), wet nitrogen (Fig. 3(B)), and dry nitrogen plus carbon dioxide (Fig. 3(C)), the *F–D* curves appear qualitatively similar to those observed for pure silica in ambient atmosphere, although the onset distances and break-free lengths occur at longer distances in the lithium silicate than the pure silica, and the attractive force is greater in the former. When the atmosphere consists of both carbon dioxide and water vapor (Fig. 3(D)), however, the *F–D* curve indicates the presence of a soft layer at the surface. In Fig. 3(D), the onset distance is several hundred angstroms before the zero approach force, and the break-free length extends beyond 700 Å (based on a higher resolution plot of the forces). A larger onset distance is indicative of either a longer range attraction between the tip and substrate atoms or a larger thickness of any overlayer liquid film on the solid substrate surface, in which the *F–D* curve shows the onset of the tip–liquid attraction. The break-free length is defined as the distance from the zero separation point on withdrawal to the point that the force again reaches zero during withdrawal. The break-free length can obviously increase with liquid overlayer thickness. The much larger onset distance and break-free length in Fig. 3(D) is attributed to the formation of a liquid contamination layer, in which these distances increase with thicker adsorbed liquid films. The smaller attractive forces measured on approach to a contaminated surface (Figs. 2(B) and 3(D)) are another consequence of the lower surface energy of the liquid contamination layer. The combined presence of water vapor and carbon dioxide apparently has a very strong effect on the reactivity of the alkali silicate surface.

To further explore the importance of water vapor, we have measured *F–D* curves for the tip contacting the lithium silicate glass in different relative humidities of nitrogen and carbon dioxide atmospheres. Figure 4 shows the average and standard deviation for 10 to 40 curves of break-free lengths for each humidity. For lithium silicate in nitrogen, the break-free length does not increase significantly until the relative humidity (RH) exceeds 40%, after which the break-free length increases sharply. This increase is attributed to an increase in the liquid layer thickness on the substrate and the capillary condensation of water around the tip while in contact with the sample. The break-free length in nitrogen is reversible on purging with dry nitrogen.

When wet carbon dioxide is used as the atmosphere in the box, the break-free length increases dramatically when the RH increases above a few percent (see Fig. 4). Pure silica does not exhibit this difference, yielding similar, and small, break-free lengths in wet carbon dioxide or nitrogen. Results similar to the behavior shown here are obtained on the other alkali silicate glasses, although the magnitude of the effect increases in the order lithium << sodium < potassium.

The increase in the adsorbed liquid film thickness observed in these AFM experiments results from the action of water on the alkali silicates and is explained as a consequence of the hygroscopicity of the glass surfaces and the partial dissolution of the alkali ions into the liquid overlayer film. Ion exchange between H_3O^+ or H^+ ions in the adsorbed overlayer liquid and alkali ions in the glass occurs rapidly. Since sodium and potassium ions have been shown to preferentially exist at the outer glass surface, whereas lithium ions do not,[3,6] the former ions are expected to react more readily and more extensively than the lithium ions. This leads to a surface hydrated layer with enhanced alkali concentration, and the ion exchange causes an

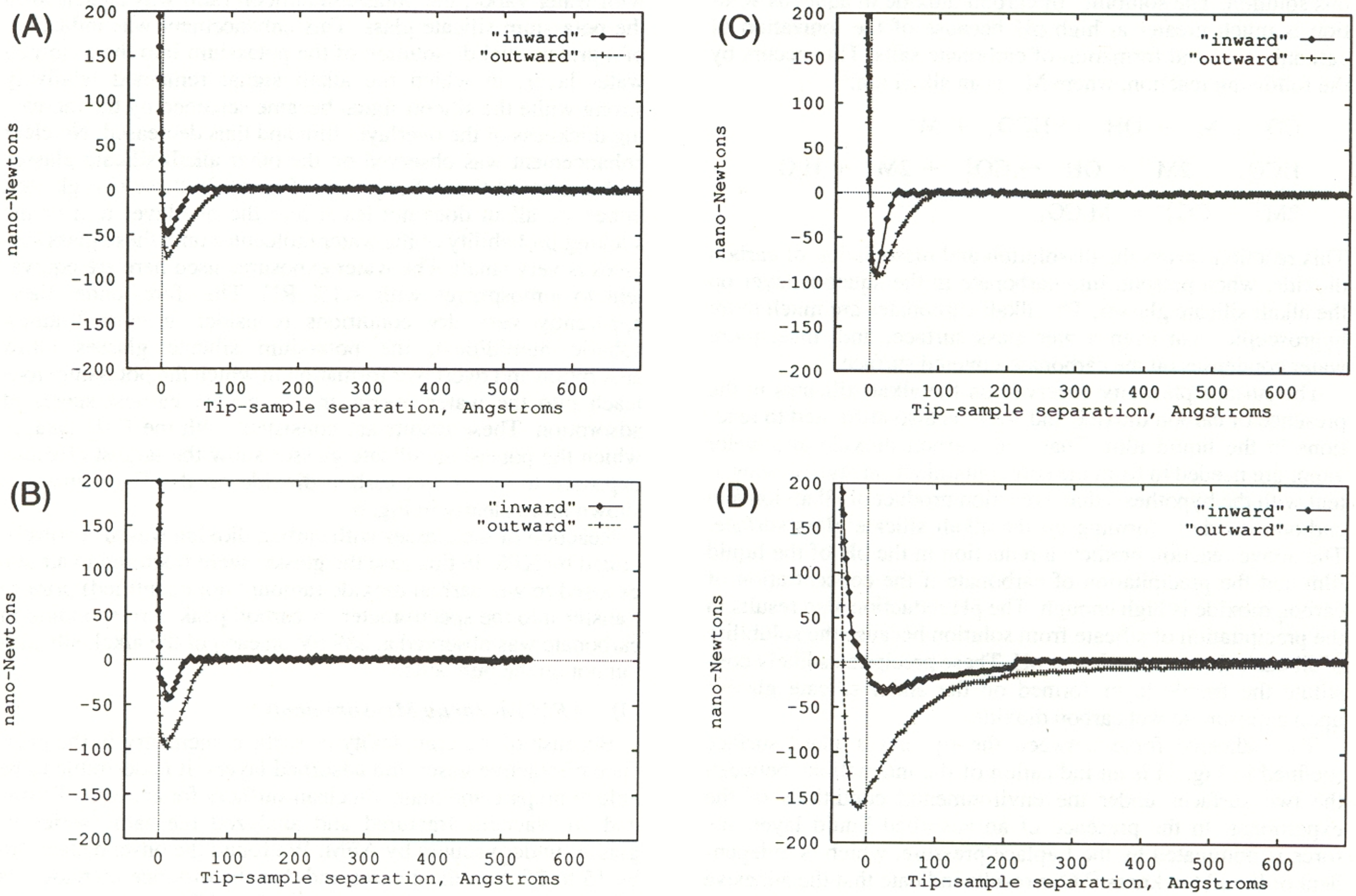

Fig. 3. Comparison of the effect of various atmospheres on the *F–D* curves for lithium silicate glass: (A) dry N_2, (B) wet N_2 (RH = 30%), (C) dry CO_2, and (D) wet CO_2 (RH = 23%).

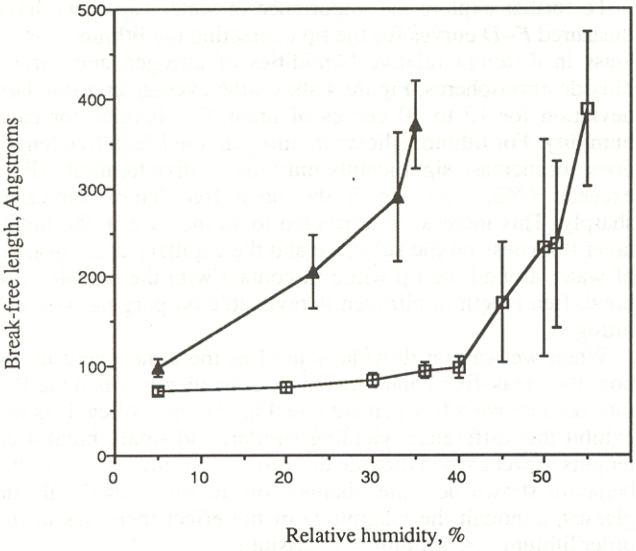

Fig. 4. Comparison of liquid film break-free lengths obtained on lithium silicate glass in (☐) N_2 and (▲) CO_2 as a function of RH.

increase in pH of the liquid water film.[21–23] In this case, alkali ions from the hydrated near-surface layer dissolve into the thin water overlayer.

The increase in break-free length in the wet carbon dioxide atmosphere suggests that the alkali silicate surfaces or the liquid film on these surfaces has a much higher affinity to water in a carbon dioxide atmosphere than in a nitrogen atmosphere. The explanation for the high affinity of alkali silicates for water in the presence of carbon dioxide is in the chemistry of the aqueous solution. The solubility of carbon dioxide in aqueous solution is much greater at high pH because of the ionization of carbonic acid and formation of carbonate salts. This occurs by the following reaction, where M^+ is an alkali ion:[24]

$$CO_2 + M^+ + OH^- \leftrightarrow HCO_3^- + M^+$$

$$HCO_3^- + 2M^+ + OH^- \leftrightarrow CO_3^{2-} + 2M^+ + H_2O$$

$$2M^+ + CO_3^{2-} \leftrightarrow M_2CO_3$$

This reaction favors the dissolution and dissociation of carbon dioxide, when present, into carbonate in the aqueous layer on the alkali silicate glasses. The alkali carbonates are much more hygroscopic than even a wet glass surface, and, thus, more water condenses on the carbonate-covered surface.

The surface plasticity observed on the alkali silicates in the presence of carbon dioxide and water is also attributed to reactions in the liquid film. That both carbon dioxide and water vapor are needed to form the soft contamination layer is consistent with the hypothesis that a reaction product of alkali ion and carbon dioxide is forming on the alkali silicate glass surface. The above reaction predicts a reduction in the pH of the liquid film and the precipitation of carbonate if the concentration of carbon dioxide is high enough. The pH reduction also results in the precipitation of silicate from solution because the solubility of silicates decreases at lower pH. These precipitates likely constitute the fragile layer formed on the alkali silicate glasses upon exposure to wet carbon dioxide.

The adhesive force between the tip and a glass surface (defined in Fig. 1) is an indication of the interactions between the two surfaces under the environmental conditions of the experiment. In the presence of an adsorbed liquid layer this force is dominated by the Laplace pressure, which is independent of liquid thickness.[25] Our results indicate that the adhesive force varies slightly or not at all with water content in a wet carbon dioxide atmosphere, even though the thickness of the liquid film increases fourfold on the alkali silicate in the RH range of <5% to 40%. Variation in the adhesive force measured on different glasses in the presence of water vapor is attributed to differences in the surface tensions of the liquid films, which are lower for the alkali silicate solutions than for pure water or carbonate solutions.[26] No viscosity effects are seen over a range of dipping rates of 1 to 100 Hz. Changes in the liquid film composition with time, glass, and vapor composition are important in determining the interfacial surface tensions. To further investigate the surface chemical reactions which can alter the liquid overlayer film composition, we have used XPS.

(2) *XPS Investigations*

The alkali silicate glasses were fractured *in vacuo* at 5×10^{-8} torr and analyzed by XPS at 2×10^{-9} torr before and after exposure to water vapor. During XPS analysis, the K 2*s*, Li 1*s*, Na 2*s* (chosen for similar escape depths), O 1*s*, C 1*s*, and Si 2*p* peaks were monitored. Molecular dynamics simulations and ion-scattering spectroscopy (ISS) experiments have previously shown segregation of potassium and sodium, but not lithium, to the outer glass surface,[3,6] with the largest alkali showing the most segregation. Corrosion of alkali silicate glasses similarly correlate with alkali-ion size, with durability decreasing in the order lithium > sodium > potassium. Prior to water vapor exposure, no clear surface enhancement of alkali was detected by XPS analysis performed here, even by making off-axis measurements. However, ISS is sensitive to the outer monolayer, and the simulations have shown rearrangements occurring in only the top 5 Å of the glasses. Since off-axis XPS averages the outer 15 Å at the energies probed, it is unlikely to detect any surface enhancement since any surface excess is compensated by a depletion of alkali about 5 to 10 Å below, minimizing any change in the signal.

The alkali/silicon ratio was monitored during exposure to water vapor, in which it was expected that the larger alkali would leach out more rapidly. After exposure of only 10^{-4} torr with water vapor, the potassium/silicon ratio was enhanced in the potassium silicate glass. This enhancement was indicative of a preferential dissolution of the potassium into the adsorbed water layer, in which the alkali signal remained relatively strong while the silicon signal became screened by the increasing thickness of the overlayer film and thus decreased. No clear enhancement was observed on the other alkali silicate glasses with increased time of exposure (Fig. 5). In these two glasses, either the alkali does not leach into the overlayer film or the sticking probability of the water molecules onto these glass surfaces is very small. The water exposures used here are equivalent to atmospheres with <1% RH. Therefore, under these apparently very dry conditions (considering normal atmospheric humidities), the potassium silicate glasses allow adsorption and overlayer formation in which the potassium ions leach into the water overlayer at the very earliest stages of adsorption. These results are consistent with the *F–D* data, in which the potassium silicate glasses show the largest effect of exposure to air or wet carbon dioxide on the *F–D* curve, as shown more clearly in Fig. 6.

Reaction of the glasses with carbon dioxide was also corroborated by XPS. In this case the glasses were fractured in air and exposed to wet carbon dioxide (amount not quantified) prior to transfer into the spectrometer. A carbon peak corresponding to carbonate was observed at 289 eV on each of the alkali silicates but not on the pure silica.

(3) *AFM In-Vacuo Measurements*

Because of the complexity of surface chemistry in the presence of reactive gases and adsorbed layers, it is desirable to be able to prepare and maintain clean surfaces for analysis. To this end we vacuum fractured and analyzed the same series of glasses under vacuum by AFM. We found the onset distance to be 15 to 25 Å in most cases and that the distance increased as silica < lithium < sodium < potassium. These values are significantly lower than those in air (see Fig. 6), especially for potassium, which goes off the scale. The short onset distance under

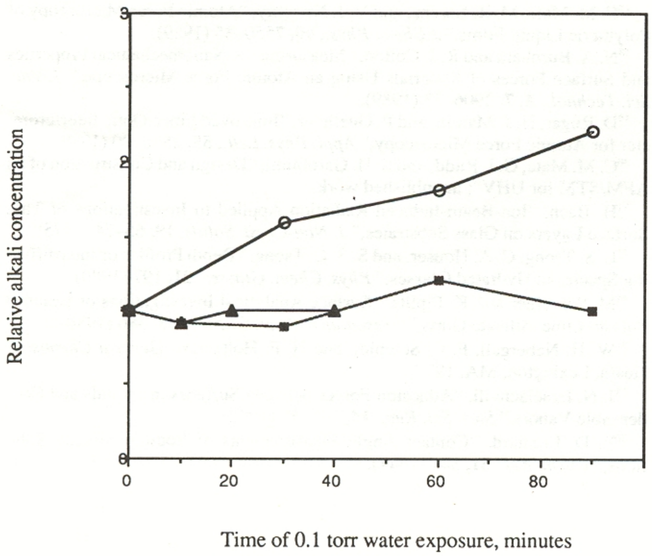

Fig. 5. Relative concentration of alkali in the respective alkali silicates as a function of water vapor exposure. Relative concentration is the ratio of the integrated intensity of the appropriate peak alkali/silicon normalized to the zero dose value. ((○) K concentration, (▲) Li concentration, and (■) Na concentration.)

vacuum indicates a surface that is free of a contamination film. Significant changes are not seen over the course of an experiment (1.5 h), indicating that adequate surface cleanliness has been maintained.

Differences between the alkali silicates and the pure silica were still observed *in vacuo*. The adhesion of the tip to the surface was consistent in the case of silica, but was higher and more variable (larger standard deviation) on the alkali silicates. Figure 7 shows a plot of the mean adhesion force and standard deviation for the experiments under vacuum. Whereas adhesion forces are dominated by the liquid film in ambient conditions, the vacuum data are indicative of the tip/glass interactions, in which the adhesion forces under vacuum are 2 to 3 times greater than those where an adsorbed liquid film is present (Figs. 1 to 3).

Another important difference between the AFM measurements made *in vacuo* and those made in other environments was the observation of variations in the F–D curves with position on the surface of the alkali silicate glasses under vacuum.

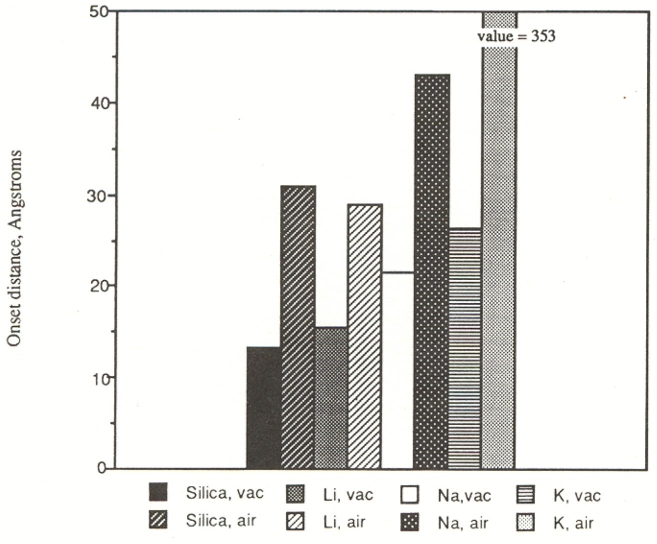

Fig. 6. Mean onset distance in air and under vacuum.

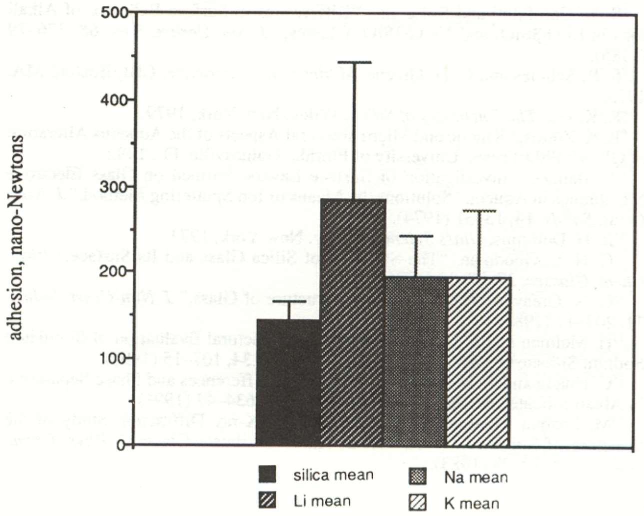

Fig. 7. Values of the adhesion force for alkali silicates fractured and analyzed *in vacuo*.

This effect, were it present on the glasses in the other environments, was apparently obscured by the magnitude of the variations caused by the environmental conditions and the adsorbed overlayer liquid. Under vacuum, however, we found detectable and reproducible differences in adhesion values on regions as close as 160 Å apart. Variations in the magnitude of onset distances and surface stiffness were also observed within a data set. The curve shape at a particular location could be reproduced by returning to the original position, thus indicating that the variations were not due to changes in tip configuration or tip contamination. Rather, these variations were indicative of heterogeneity on this scale. Based on the nanoscale heterogeneity in alkali silicate glasses inferred from experiments[12,13] and observed in simulations,[14,15] this heterogeneity was probably due to compositional variations. Such variations existed on lithium, sodium, and potassium silicate glasses but not on pure silica.

IV. Conclusion

AFM measurements demonstrate that the 30 mol% alkali silicate glasses react with water vapor and carbon dioxide in the order lithium << sodium < potassium. XPS shows that water induces surface segregation and leaching of potassium on the potassium silicate glass even at less than <1% RH. XPS also yields evidence of formation of alkali carbonate on alkali glasses at the onset of exposure to wet carbon dioxide. AFM detects a thin liquid layer formed on exposure to water vapor, and reaction of this layer with carbon dioxide results in formation of a plastic layer in the glass which is not removed by subsequent exposure to a dry atmosphere. AFM *in vacuo* indicates that the fracture surfaces of the 30 mol% alkali silicate glasses are spatially heterogeneous; no such heterogeneity is observed on pure silica. This heterogeneity is believed to be due to variations in the composition of alkali silicate glasses on the nanometer and subnanometer scale.

References

[1] A. Paul, *Chemistry of Glasses*. Chapman Hall, London, U.K., 1982.

[2] F. R. Bacon, "The Chemical Durability of Glass, Part One," *Glass Ind.*, 438–46 (1968).

[3] C. P. Pantano, J. F. Kelso, and M. J. Suscavage, *Advances in Materials Characterization*; pp. 1–38. Plenum Press, New York, 1983.

[4] R. Bruckner, H.-U. Chun, and H. Goretzki, "Photoelectron Spectroscopy (ESCA) on Alkali Silicate and Soda Aluminosilicate Glasses," *Glastech. Ber.*, **51,** 1–7 (1978).

[5] J. S. Jen and M. R. Kalinowski, "An ESCA Study of the Bridging to Non-Bridging Oxygen Ratio in Sodium Silicate Glass and the Correlations to Glass Density and Refractive Index," *J. Non-Cryst. Solids*, **38 & 39,** 21–26 (1979).

[6]S. H. Garofalini and S. Levine, "Differences in Surface Behavior of Alkali Ions in $Li_2O{\cdot}3SiO_2$ and $Na_2O{\cdot}3SiO_2$ Glasses," *J. Am. Ceram. Soc.*, **68,** 376–79 (1985).

[7]S. R. Scholes and C. H. Greene, *Modern Glass Practice*. CBI, Boston, MA, 1975.

[8]R. K. Iler, *The Chemistry of Silica*. Wiley, New York, 1979.

[9]B. K. Zoitos, "Kinetic and Microstructural Aspects of the Aqueous Alteration of Glass"; PhD Thesis. University of Florida, Gainesville, FL, 1992.

[10]F. Baucke, "Investigation of Surface Layers, Formed on Glass Electrode Membranes in Aqueous Solutions, by Means of Ion Sputtering Method," *J. Non-Cryst. Solids*, **14,** 13–31 (1974).

[11]R. H. Doremus, *Glass Science*. Wiley, New York, 1973.

[12]C. H. L. Goodman, "The Structure of Silica Glass and Its Surface," *Phys. Chem. Glasses*, **27,** 27–31 (1986).

[13]G. N. Greaves, "EXAFS and the Structure of Glass," *J. Non-Cryst. Solids*, **71,** 203–17 (1985).

[14]H. Melman and S. H. Garofalini, "Microstructural Evaluation of Simulated Sodium Silicate Glasses," *J. Non-Cryst. Solids*, **134,** 107–15 (1991).

[15]C. Huang and A. N. Cormack, "Structural Differences and Phase Separation in Alkali Silicate Glasses," *J. Chem. Phys.*, **95,** 3634–42 (1991).

[16]M. Imaoka, H. Hasegawa, and I. Yasui, "X-ray Diffraction Study of the Structure of Silicate Glasses. Part 2. Alkali Disilicate Glasses," *Phys. Chem. Glasses*, **24,** 72–78 (1983).

[17]C. M. Mate, M. R. Lorenz, and V. J. Novotny, "Atomic Force Microscopy of Polymeric Liquid Films," *J.Chem. Phys.*, **90,** 7550–55 (1989).

[18]N. A. Burnham and R. J. Colton, "Measuring the Nanomechanical Properties and Surface Forces of Materials Using an Atomic Force Microscope," *J. Vac. Sci. Technol., A*, **7,** 2906–13 (1989).

[19]D. Rugar, H. J. Mamin, and P. Guethner, "Improved Fiber-Optic Interferometer for Atomic Force Microscopy," *Appl. Phys. Lett.*; **55,** 2588–90 (1989).

[20]C. M. Mate, G. I. Rudd, and S. H. Garofalini, "Design and Construction of an AFM/STM for UHV"; unpublished work.

[21]H. Bach, "Ion-Beam-Induced Radiation Applied to Investigations of Thin Surface Layers on Glass Substrates," *J. Non-Cryst. Solids*, **19,** 65–74 (1975).

[22]L. S. Tsong, C. A. Houser, and S. S. C. Tsong, "Depth Profiles of Interdiffusing Species in Hydrated Glasses," *Phys. Chem. Glasses*, **21,** 197 (1980).

[23]M. Schreiner and K. Piplits, "Surface Analytical Investigations of Leached Potash–Lime–Silicate Glass," *Fresenius Z. Anal. Chem.*, **333,** 386 (1989).

[24]W. H. Nebergall, F. C. Schmidt, and H. F. Holtzclaw, *General Chemistry*. Heath, Lexington, MA, 1972.

[25]J. N. Israelachvili, "Adhesion Forces between Surfaces in Liquids and Condensable Vapors," *Surf. Sci. Rep.*, **14,** 109–59 (1992).

[26]P. D. Liddiard, "Contact Angle Measurements of Sodium Silicate Solutions," *Chem. Age*, **51,** 341 (1944). ☐